

Complexing mercuric oxide sols by acetone

Christian Bonhomme, Marc Henry and Jacques Livage

Laboratoire de Chimie de la Matière Condensée, Université Pierre et Marie Curie, 4 place Jussieu, 75252 Paris cédex 05, France

Received 7 August 1992

Revised manuscript received 25 November 1992

Stable mercuric oxide sols have been obtained by adding aqueous HgCl_2 solutions to KOH (aq) in the presence of acetone. Very small globular colloidal particles ≈ 5 nm in diameter are formed after a critical time which depends on the amount of acetone. These sols undergo a sol–gel transition upon aging at 80°C . Spectroscopic characterizations of the sols, gels and xerogels show that acetone molecules interact strongly with Hg atoms at the surface and/or the core of the particles. These interactions involve both the carbonyl group via donor–acceptor covalent bonds and the methyl group via the formation of stable $\text{Hg}-\text{CH}_2-$ bonds. These amorphous colloids could therefore be described as hybrid organic–inorganic compounds. Their broad size distribution and amorphous structure precludes the observation of quantum size effects but they could open new possibilities for the sol–gel synthesis of novel hybrid materials.

1. Introduction

The sol–gel process is a new, appealing way to obtain glasses and ceramics [1]. Research in this field mainly involves the hydrolysis and condensation of metal alkoxides [$\text{Si}(\text{OR})_4$, $\text{Al}(\text{OR})_3$...] in the presence of various organic additives and solvents [2]. Aqueous solutions of metal salts (chlorides, nitrates...) are also currently used in industry for the precipitation of oxide powders. Molecular precursors are then aquo cations or oxo-anions. Hydrolysis and condensation are obtained by changing the pH [3] or raising the temperature [4]. With the growing interest in new materials from molecular precursors, the sol–gel process is moving towards the synthesis of hybrid organic–inorganic materials [5]. Chemical modification of molecular precursors by organic and/or inorganic reagents provides functionalized species which would lead to strong modifications of the

structure and texture of the oxide network. It appears that one of the most promising ways to obtain new materials with optimized properties lies in the ability to perform both organic and inorganic polymerization. In the case of silicon-based materials, organic functionalization is achieved by replacing Si–OR bonds by Si–R bonds, which remain stable upon hydrolysis [6]. For transition-metal-based materials, hydrolysis of the M–C bonds occurs and complexing ligands (organic acids, β -diketones, polyols, etc.) have to be used [7]. The strong reactivity of M–C bonds towards water is related to the low electronegativity of transition metals relative to carbon ($\chi_{\text{C}} = 2.5$ on the Allred–Rochow scale). The higher electronegativity of silicon ($\chi_{\text{Si}} = 1.74$) leads to more covalent Si–C bonds, which remain stable in the presence of water. Other atoms, such as mercury, have electronegativities ($\chi_{\text{Hg}} = 1.80$) close to that of silicon. Covalent Hg–C bonds should therefore be stable towards hydrolysis. Another reason for studying HgO-based colloids is that they can be stabilized by organic additives such as acetone [8] but, to our knowledge, this has never been explained on a molecular basis. This work presents

Correspondence to: Dr C. Bonhomme, Laboratoire de Chimie de la Matière Condensée, Université Pierre et Marie Curie, T54-55, 5 étage, 4 place Jussieu, 75252 Paris cédex 05, France. Tel: +33-144273365. Telefax: +33-144274769.

a detailed molecular analysis of chemical interactions of such colloids with acetone and inorganic counter-ions.

2. Experimental

Mercuric oxide sols were prepared according to the literature [8]. A saturated aqueous HgCl_2 solution ($[\text{Hg}^{2+}] = 0.25 \text{ M}$) was added dropwise, at room temperature with stirring, to a KOH solution (10 ml; 1 M; $\text{pH} \approx 14$) containing acetone (4 vol%; 0.4 ml). After each drop a yellow precipitate formed which dissolved into the solution. At the end, a clear and colorless solution was obtained. This solution slowly becomes turbid, giving a pale yellow gel upon aging at room temperature.

Transmission electron microscopy (TEM) micrographs and diffraction patterns were obtained with a JEOL 100 CXII electron microscope. Samples were prepared by evaporating onto carbon-coated grids either sols, ultrasonicated aqueous dilutions of gels or aqueous suspensions of fine xerogel powders. Lattice-spacing were calibrated using a gold diffraction pattern. The particle size distribution was estimated by measuring about 500 particles.

Quasielastic light scattering (QLS) was used to obtain the mean diffusion coefficient, D , of the scattering particles. A Spectra-Physics He-Ne Laser ($\lambda = 6328 \text{ \AA}$), operating at 5 mW, was used in conjunction with a digital Brookhaven autocorrelator. The autocorrelation function was analyzed using a non-negatively constrained least-squares analysis. From D , the mean hydrodynamic radius, R_h , is obtained, using the Stokes-Einstein equation: $R_h = kT/6\pi\eta D$, with k Boltzmann's constant, T absolute temperature and η the solvent viscosity.

UV spectroscopy was performed on solutions using a Kontron Uvikon 860 (180–400 nm) spectrometer (quartz cells: 1 cm). Xerogels were analyzed by FTIR spectroscopy using a UFS 45 Bruker spectrometer (400–4000 cm^{-1}). Both liquid and solid samples were investigated by Raman spectroscopy with a Jobin-Yvon U1000 double monochromator spectrometer with a continuous wave Ar^+ coherent laser ($P = 80 \text{ mW}$).

X-ray diffraction patterns were recorded on a Philips PW 18–20 powder diffractometer equipped with a graphite monochromator, using the $\text{Cu K}\alpha$ radiation ($\lambda = 1.54186 \text{ \AA}$).

Cross-polarized magic angle spinning (CP MAS) ^{13}C solid-state NMR spectra of the xerogels were recorded on a Bruker MSL 400 spectrometer, using a TOSS program in order to suppress the spinning side-bands. Pulse width and relaxation delays were 5.4 μs and 5 s (contact time: 1.5 ms) respectively. Solid samples were spun at 3 kHz.

3. Results

The evolution of the sols described above depends on several parameters. The gelation time decreases rapidly when the temperature increases. It occurs after more than 50 h at 35°C and 2 h at 80°C.

Three main chemical parameters seem to be important for the sol-gel transition.

(i) The ratio $h = [\text{OH}^-]/[\text{Hg}^{2+}]$. Depending on h , either gelatinous precipitates ($h \geq 4$ or $h \leq 2$), turbid liquids ($3 \leq h \leq 4$) or stable colloidal solutions ($2 \leq h \leq 3$, after 40 h aging) are obtained. The most stable solutions which remain clear and colorless for weeks are obtained for $h = 2.25$ (or $[\text{Hg}^{2+}] = 0.16 \text{ M}$). All gelatinous precipitates lead to yellow gels when heated a few hours at 80°C.

(ii) The volume fraction of acetone $V = \text{acetone}/\text{H}_2\text{O}$ in the aqueous solution. At a given temperature, the gelation time increases with the amount of acetone. For $T = 60^\circ\text{C}$ and $h = 2.25$, gelation is observed after 2 h for $V = 2\%$ and 10 h for $V = 12\%$. Sols can not be stabilized for very low volume fractions ($V < 2\%$) and precipitation occurs. In the absence of acetone, an orange/yellow precipitate of HgO (montroydite) is obtained.

(iii) The inorganic counter-ion. Stable sols cannot be obtained when aqueous solutions of mercuric nitrate are used [$\text{Hg}(\text{NO}_3)_2$, H_2O , 0.25M in $\text{H}_2\text{O}/\text{HNO}_3$] for $[\text{Hg}^{2+}] > 0.04\text{M}$. However adding chloride ions (for instance by dissolving a given amount of KCl 0.5M) leads to the formation of stable sols which give rise to gels upon aging.

A detailed investigation of the system was carried out for $h = 2.25$ (or $[\text{Hg}^{2+}] = 0.16\text{M}$, $[\text{Cl}^-] = 0.32\text{M}$ and $V = \text{acetone}/\text{H}_2\text{O} = 4\%$):

As-prepared sols consist of large particles ($\approx 48\text{ nm}$ in diameter) mixed with much smaller particles ($\approx 5\text{ nm}$ in diameter), both having roughly spherical shapes (fig. 1(a)). Dispersed gels obtained upon aging in water also shows globular particles (fig. 1(b)) with a rather broad size distribution (fig. 2) and a mean diameter $\approx 4.8\text{ nm}$. Electron diffraction patterns of these gels show only diffuse rings. The first one corresponds to a d -spacing of about 2.9 \AA . The electron micrograph of xerogel powders is presented in fig. 1(c). Larger globular particles with a mean diameter $\approx 8\text{ nm}$ are observed in the xerogel powder (fig.

1(c)). Chemical analysis by EDAX shows that they mainly contain Hg and Cl atoms.

Light scattering experiments provide information about the size and shape of the colloidal particles. The mean hydrodynamic diameter of the particles was measured as a function of time without dilution of the samples (fig. 3). The mean diameter first increases with time and then suddenly decreases after a critical time ($t_c \approx 10\text{ h}$) to a mean value of about 5 nm . A distribution size analysis is presented in fig. 2. Comparison of the size distribution with the TEM results indicates that both measurements are in rough agreement, except for very small particles ($< 4\text{ nm}$ in diameter). We assume, in the present case, that it is possible to compare a diameter measured directly

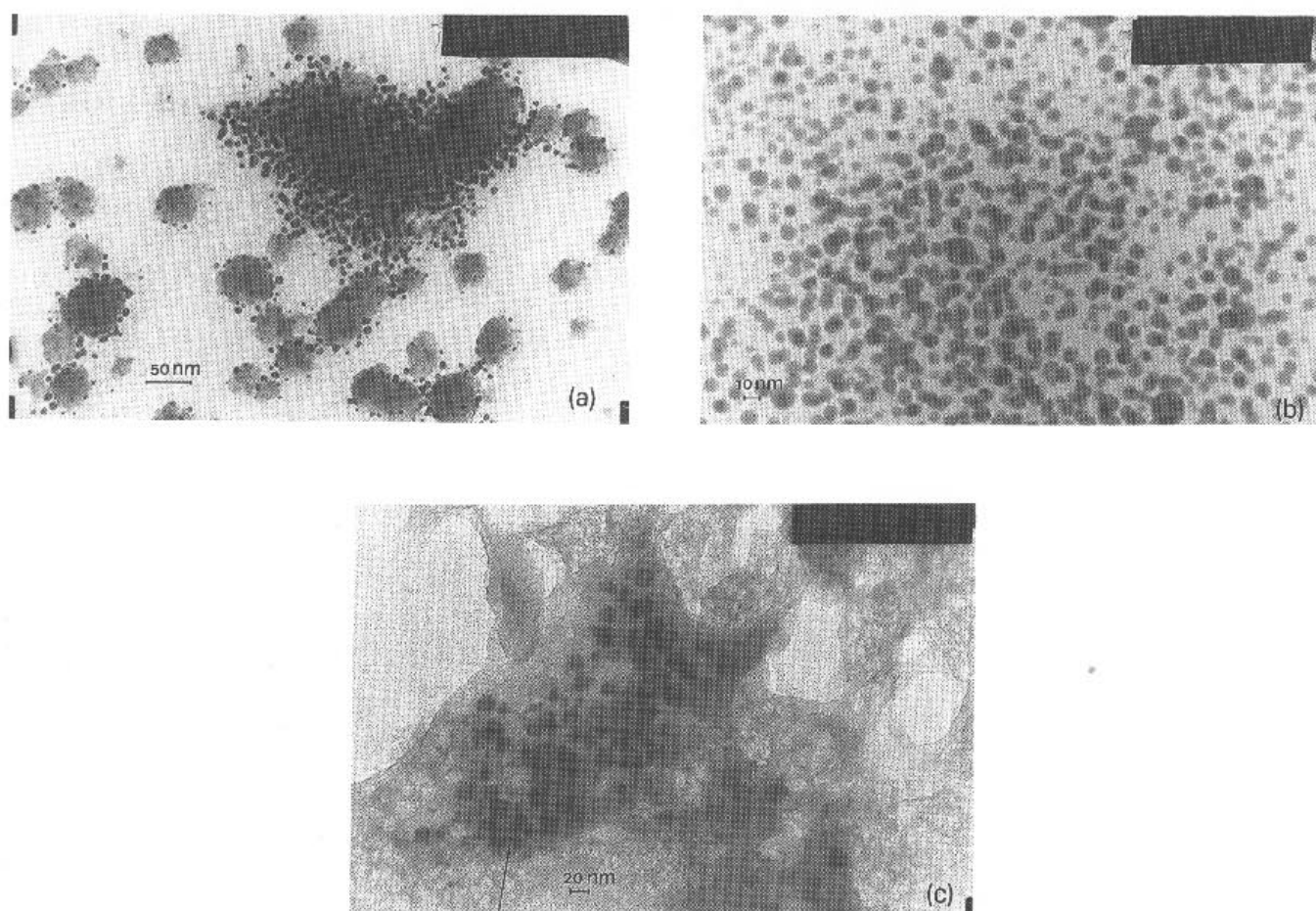


Fig. 1. (a) TEM micrograph of a sol ($h = 2.25$) (without aging); (b) TEM micrograph of a gel ($h = 2.25$) (dilution in water); (c) TEM micrograph of a xerogel ($h = 2.25$) (dispersion in water).

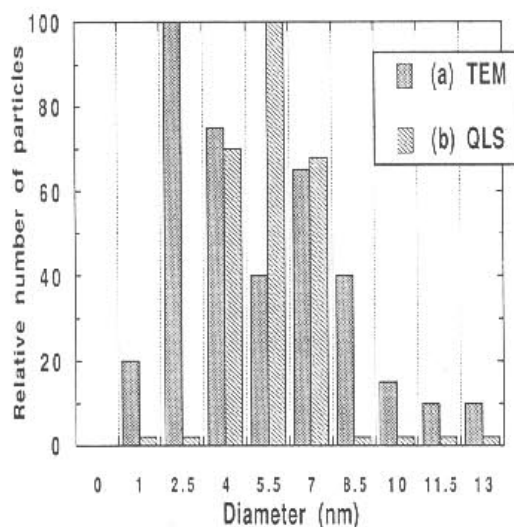


Fig. 2. Particles size distribution obtained by TEM experiments (a) and QLS (b).

on a micrograph and a hydrodynamic diameter, the shape of the particles being nearly spheroidal.

The diameter of the colloidal particles does not exceed 1/20th of the wavelength of the incident light ($\lambda = 632.8$ nm). They behave as Rayleigh scatterers and it is not possible to deduce information about the shape of these particles from static light scattering measurements.

Sols corresponding to different values of h were analyzed by Raman spectroscopy (fig. 4). Increasing Hg^{2+} concentration leads to a decrease of the relative intensity of Raman bands at

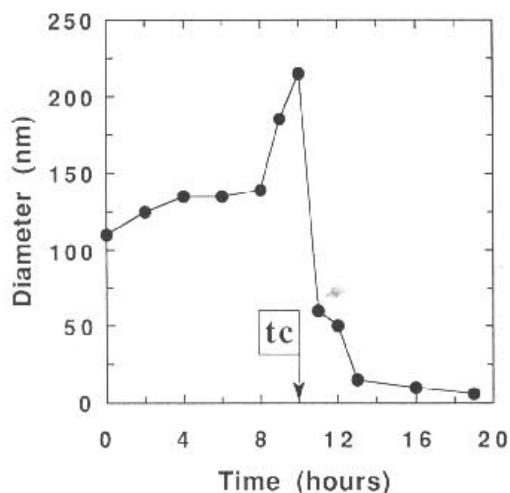


Fig. 3. Evolution with time of the mean hydrodynamic diameter of particles in the sols ($h = 2.25$).

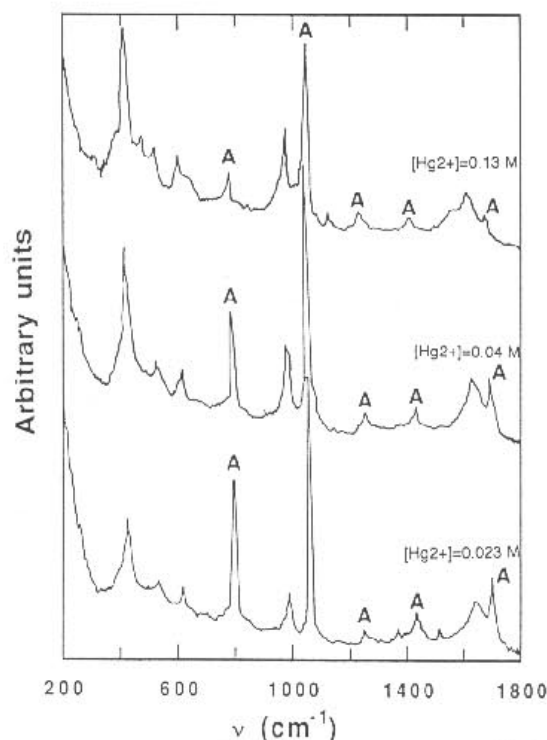


Fig. 4. Raman spectra of the sols: influence of $[\text{Hg}^{2+}]$. Free acetone bands are labeled A (see table 1).

$\nu = 800$ cm^{-1} , $\nu = 1701$ cm^{-1} while new bands appear at $\nu = 440, 504, 550, 624, 990$ and 1680 cm^{-1} .

Sols prepared from $\text{Hg}(\text{NO}_3)_2$ {for $[\text{Hg}^{2+}] < 4 \times 10^{-2}$ M} were also analyzed by Raman spectroscopy. They lead to the same observations, i.e. a decrease of the same Raman bands and the appearance of new bands at positions as above.

Raman spectra of xerogel and precipitates (obtained with mercury nitrate) are presented in fig. 5. Similar spectra are observed for solid and liquid samples, although some shifts of Raman bands are observed ($624 \rightarrow 674$; $1680 \rightarrow 1550$; 990 and $1060 \rightarrow 1045$ cm^{-1}). The spectra of solid samples are better resolved and it is possible to observe three new bands at $254, 312$ and 350 cm^{-1} . Precipitates obtained with $\text{Hg}(\text{NO}_3)_2$ lead to the same conclusions, new bands are observed at $252, 287$ and 317 cm^{-1} .

FTIR spectra of the xerogel obtained for $[\text{Hg}^{2+}] = 0.16$ M were recorded to correlate both IR and Raman vibrational information. A summary of the Raman and IR bands observed for both solutions and solids is given in table 1.

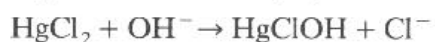
The UV spectrum of an aqueous solution of HgCl_2 with acetone (4 vol%) (fig. 6(a)) shows an intense band at 200 nm ($\epsilon \approx 5000$). Sols ($h = 2.25$) show the same band ($\lambda_{\text{max}} = 200$ nm) with a weak shoulder around $\lambda_{\text{max}} \approx 250$ nm (fig. 6(b)). This shoulder increases in intensity upon aging.

X-ray diffraction patterns of xerogels and precipitates (fig. 7) show that these samples are very poorly crystallized. Only two broad peaks can be seen which correspond approximately to $d \approx 2.7$ Å and $d \approx 1.7$ Å. They seem to correspond to the envelope of the main diffraction peaks of HgO (montroydite) which is obtained by the base hydrolysis of aqueous HgCl_2 without acetone.

The ^{13}C CPMAS spectrum of the xerogel ($h = 2.25$) shows five broad peaks at $\delta = 36, 54, 80, 117$ and 217 ppm (fig. 8).

4. Discussion

It is well known that the base hydrolysis of a HgCl_2 solution leads to $\text{Hg}(\text{OH})_2$ species according to the reactions [11]



No proton transfer seems to occur between the hydrated cation and the hydroxide ion OH^- . KOH in excess prevents the formation of oxychlorides species in the solution. Once formed $\text{Hg}(\text{OH})_2$ species rapidly transform onto the oxide HgO . The redissolution of this oxide occurs when acetone is present in the KOH solution.

Electron and X-ray diffraction of the xerogels (fig. 7) show that all materials investigated are

Table 1
Observed frequencies for the Raman and FTIR spectra of sols, xerogel ($h = 2.25$) and precipitate obtained with mercury nitrate

Sols (Raman) (cm^{-1})	Xerogel (Raman) (cm^{-1})	Xerogel (IR) (cm^{-1})	Precip. (Raman) (cm^{-1})	Proposed assignments
	254 m		252 m	Hg-O str
			287 sh	
	312 m		317 m	Hg-O str
328 vw	349 m			Hg-Cl str
440 s	452 s		448 s	Hg-C str
506 w	506 s	502 w, br	502 s	Hg-O str
545 w	544 s		547 s	Hg-C str (+ C=O def)
624 m		641 w		?
	672 m		674 m	Hg-O-Hg str + CH=def
	747 m, br	752 w	750 br	
800 s-w		888 sh		CC_2 sym str
	920 m		925 w	OH def
993 s				CH_2 def
			1039 s	NO_3 str
1065 s	1044 s	1047 m	1040 s, br	CH_3 def (A)
1148 w	1152 w	1129 w	1130 w	CH_2 def
1240 w	1260 w	1208 s	1250 w	CC_2 asym str
		1317 w		CH_3 def
1430 w	1413 w	1410 w	1414 w	CH_3 def
1561 br	1539 m, br	1507 s	1590 m, br	C=C str + (C=O str)
1630 m, br				C=O str
1701 w				C=O str (A)
		2922 w		CH str
		3427 m, br		OH str

s = strong intensity; v = very; m = medium; w = weak; br = broad, sh = shoulder; sym = symmetric; asym = asymmetric; def = deformation, str = stretch.

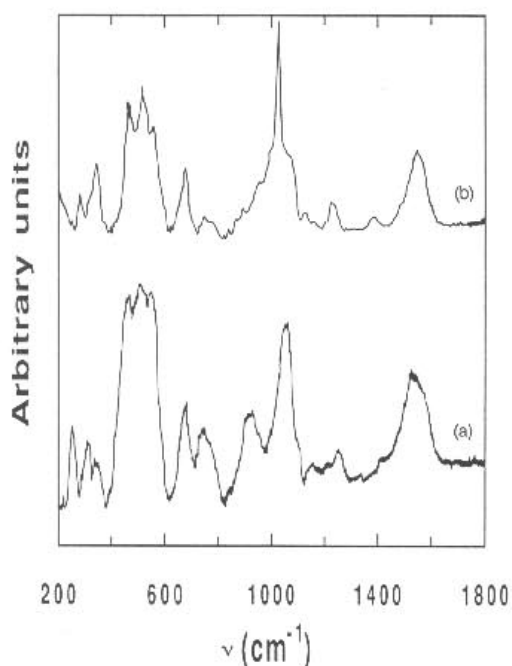


Fig. 5. Raman spectra of the xerogel ($h = 2.25$) (a) and precipitate (b) obtained with mercury nitrate.

amorphous. Some correlations can be found between the position of the broad peaks and the diffraction pattern of crystalline HgO suggesting that xerogels exhibit some long-range order close to that of HgO. The redissolution of the yellow mercuric oxide in the presence of acetone (lead-

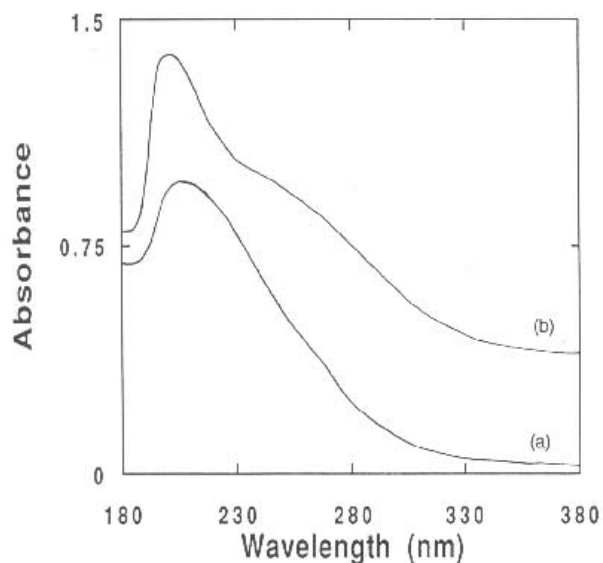


Fig. 6. UV spectra of an aqueous solution of HgCl_2 with acetone (4 vol.%) (a) and of sol ($h = 2.25$) (b).

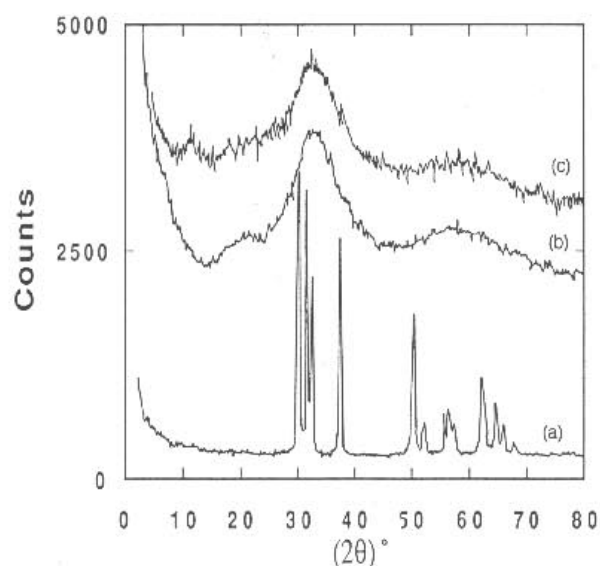


Fig. 7. Diffraction pattern of mercuric oxide HgO (montroydite) (a), xerogel ($h = 2.25$) (b) and precipitate obtained with mercury nitrate (c).

ing to colloidal particles) can then be described as a complexing process by acetone molecules assisted by Cl^- ions.

Raman bands were assigned according to the literature [12–15] and a Raman study of a reference system described by Johnson and Perry [16]. These authors used ^1H and ^{199}Hg NMR spectroscopy to investigate the mercuration (and polymerization) of acetone in acidic aqueous solu-

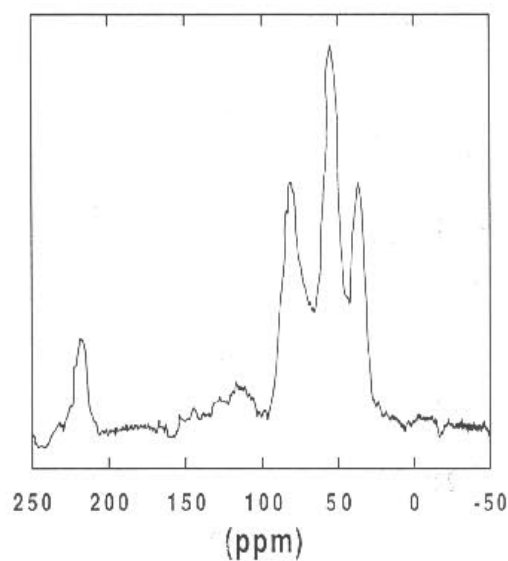
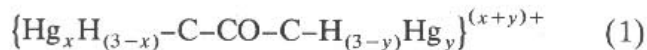


Fig. 8. ^{13}C CPMAS NMR spectrum of a xerogel sample ($h = 2.25$).

tions of $\text{Hg}(\text{NO}_3)_2$. NMR spectra show that nine mercurated acetone species are in equilibrium. They correspond to



(x and y change from 1 to 3 with time).

The evolution with time of the Raman spectra is presented in fig. 9. Proposed assignments are listed in table 2, assuming the formation of the species described by eq. (1) and according to ref. [17]. The vibrations bands of NO_3 groups are well known [15] and are labeled N in fig. 9. Free acetone molecules bands are labeled A. The bands centered at 440 cm^{-1} ($\nu\text{Hg}-\text{C}$), 550 cm^{-1} ($\nu\text{Hg}-\text{C}$), 620 , 1100 and 1660 cm^{-1} have been observed by many authors and are characteristic of mercurated aldehydes and ketones [13].

Raman spectra of the sols (fig. 4) show that some acetone molecules react with Hg during the redissolution of mercuric oxide. The species produced by this mercuration (or polymercuration) reaction are characterized by Raman bands centered at 440 , 550 , 624 , 990 and 1680 cm^{-1} . Their formation leads to a decrease of the Raman

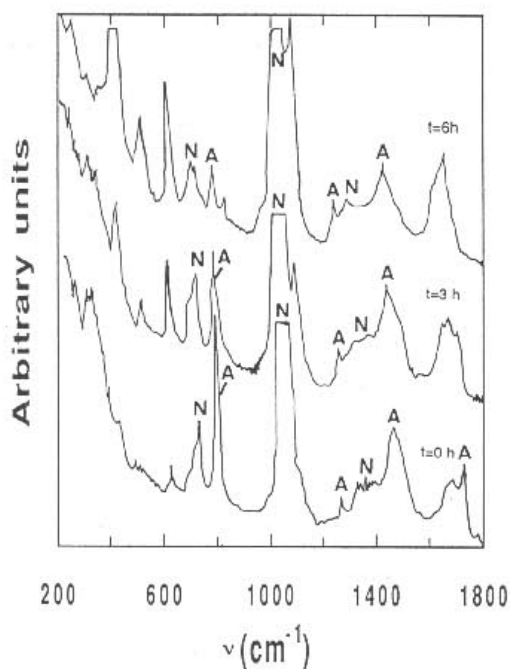


Fig. 9. Evolution with time (hours) of the Raman spectra of a mercury (II) nitrate/acetone system [15].

Table 2
Observed frequencies for Raman spectra of a mercury (II)/acetone system [15]

(Raman) (cm^{-1})	Proposed assignments
287 m	
455 s	Hg-C str
548 m	Hg-C str
640 m	?
715 w	NO_3 str
739 w	NO_3 str
801 s	CC_2 sym str
836 w	
1050 vs	NO_3 str + def CH_3 (A)
1100 s	CH_2 def
1250 w	CC_2 asym str
1310 br	CH_3 def + NO_3 str
1435 br	CH_3 def + NO_3 str
1649 m, br	C=O str
1701 w	C=O str (A)

Abbreviations as in table 1.

bands of free acetone (labeled A): CC_2 symmetrical stretch ($\nu = 800 \text{ cm}^{-1}$), C=O stretch ($\nu = 1701 \text{ cm}^{-1}$) [9]. A band centered at 504 cm^{-1} , which does not appear in the spectra of mercurated acetone in acidic solutions (fig. 9), is also observed and could be assigned to a Hg-O stretching vibration [15]. However, the low value observed for the Hg-C stretching vibration (440 cm^{-1}) suggests that polymeric $-\text{C}-\text{Hg}-\text{C}-$ species are formed. Such values have already been observed for $(\text{RCH}_2)_2\text{Hg}$ organomercury compounds [12] and for mercury β -diketonato complexes [25]. In both cases $-\text{C}-\text{Hg}-\text{C}-$ bonds are involved. The formation of $-\text{C}-\text{Hg}-\text{X}-$ ($\text{X} = \text{Cl}$) bonds cannot be excluded, especially for the highest values of $[\text{Hg}^{2+}]$. The band centered at 328 cm^{-1} could be assigned to Hg-Cl stretching vibrations.

A strong shift, typical of the stretching vibration band of carbonyl groups interacting with Hg atoms, is observed [18]. Such interactions have been suggested and confirmed by crystallographic studies on mercurated ketones [18,19]. This suggests that the mercurated species formed by the redissolution of mercuric oxide belong to a solid phase, i.e. the colloidal particles.

The presence of such species is also shown by UV spectroscopy (fig. 6). The shoulder at 250 nm is in agreement with values reported for other mercurated compounds [20].

The yield of mercuration does not appear to be quantitative. Free acetone remains in the solution for the highest values of $[\text{Hg}^{2+}]$. It can be characterized by the C–C–C symmetrical stretch ($\nu = 800 \text{ cm}^{-1}$). Finally stable colloids (mean diameter $\approx 5 \text{ nm}$) are obtained which contain both mercuric oxide and organomercury phases. The stability of these sols is ensured by both acetone molecules and chloride ions which are known to be strong complexing agents of Hg^{2+} ions [11]. The presence of Cl^- ions bonded to mercury atoms is evidenced by UV spectroscopy of the sol ($\lambda_{\text{max}} = 200 \text{ nm}$, $\epsilon \approx 5000$) [10] (fig. 6).

^1H and ^{13}C NMR experiments on the sol show that acetone molecules are located near the surface of the colloids. NMR signals decrease in intensity when $[\text{Hg}^{2+}]$ increases, i.e. when the amount of solid phase increases in the sols. The chemical shifts observed in ^1H NMR (related to TMS) are: $\delta = 2.01, 2.11$ and 2.34 ppm . They can be assigned to the protons of methyl groups of either free acetone molecules ($\delta = 2.01 \text{ ppm}$) or mono- and di-mercurated species ($\delta = 2.11$ and 2.34 ppm). Such chemical shifts have been observed by Johnson and Perry [16]. ^{13}C NMR experiments lead to poorly resolved spectra with a low signal-to-noise ratio.

The position of the mercurated species, inside or at the surface of colloidal particles, remains unclear. Raman and FTIR analysis of xerogels (and precipitates) (fig. 5 and table 1) suggest strong similarities between sols and xerogels. Both Hg–C ($\nu = 452, 544 \text{ cm}^{-1}$) and Hg–O vibrations ($\nu = 253, 312, 506 \text{ cm}^{-1}$) [15] are present. Several differences should, however, be pointed out.

(1) No C–C–C stretching vibration band ($\nu = 800 \text{ cm}^{-1}$) can be detected, suggesting that free acetone molecules are not trapped in the xerogel.

(2) A strong shift to lower wavenumbers of the C=O stretching vibration band ($1680 \text{ cm}^{-1} \rightarrow 1539 \text{ cm}^{-1}$) is observed. This shift could be due to the formation of C=C double bonds. This hypothesis is confirmed by ^{13}C CPMAS experiments on the xerogel ($h = 2.25$) (fig. 8). The broad peak at 117

ppm is typical of sp^2 carbon atoms. These new species could result from the condensation (favorable in alkaline media and in the presence of oxide [21]) of two acetone molecules, leading to a $-\text{CO}-\text{C}=\text{C}-$ group.

(3) The band at 672 cm^{-1} , which is observed in the solid state, could be associated with an organo-oxide vibration (C–Hg–O–Hg–C). This low-frequency region is indeed characteristic of oxo groups bridging two organo 'heavy' metallic species [22]. This band could also be assigned to a $\gamma(\text{CH}=\text{C})$ deformation vibration which appears to be characteristic of allyl mercury compounds [14].

(4) The presence of OH vibration bands (IR 3427 cm^{-1} , Raman: 920 cm^{-1}) may correspond to water molecules or OH groups (i.e. $-\text{Hg}-\text{OH}-\text{Hg}$) in the xerogel. This correlates with the presence of a Raman band centered at 506 cm^{-1} [15].

The sol-gel transition arises from the evaporation of free-acetone and water together with condensation reactions. This leads to aggregation of colloidal particles which appears to remain unchanged in the xerogel (fig. 1(c)). A hybrid organic-inorganic network, containing Hg–O and Hg–C bonds should be formed. These modifications are clearly seen in the NMR ^{13}C CPMAS spectrum of the xerogel (fig. 8). NMR peaks centered at 36, 117 and 214 ppm can be easily assigned to CH_3 , C=C and C=O groups. Other peaks at 54 and 80 ppm can be related to organomercury species containing both C=C and C=O bonds [23,24]. The absence of signals around 170–180 ppm excludes the presence of carboxylate species which could result from redox reactions involving acetone and mercury.

5. Conclusions

Stable colloidal solutions containing HgO-based particles with a mean diameter close to 5 nm have been obtained. Such colloids are not readily obtained immediately after adding the metal salt to the base solution. They are formed upon aging the mother solution for several hours. Raising the temperature promotes dispersion of large colloidal aggregates but also favors a non-

reversible sol-gel transition. The chemical role of both acetone molecules and chloride ions in this process has been clearly evidenced. Two kinds of interactions have been characterized:

(i) a donor-acceptor type interaction $C=O \rightarrow Hg$ where acetone molecules keep their integrity.

(ii) a covalent bond $Hg-CH_2-CO-CH_3$ through the mercuration of methyl groups. The presence of methyl groups around the carbonyl group appears to be important as stabilization is much reduced when cyclopentanone is used in place of acetone.

Mercuration reactions of aldehydes and ketones are well known from organometallic chemists. Most interestingly β -diketones such as acetylacetone (acacH) can also be mercured but at the methylene carbon rather than the OH group. This mercuration reaction opens new opportunities for the sol-gel synthesis of novel hybrid materials:

(i) the functionalization of silicon alkoxide by acetone $(RO)_3Si-CH_2-CO-CH_3$ and subsequent mercuration of the remaining methyl groups would lead to hybrid organic-inorganic materials containing both Hg-C and Si-C bonds.

(ii) the functionalization of transition metal alkoxides $M(OR)_n$ with the enol form of acacH, followed by mercuration at the methylene carbon atom, would lead to another kind of hybrid organic-inorganic network containing both Hg-C and M-O bonds.

Obviously, if acetone or acacH are functionalized before reacting with $Si(OR)_4$ and $M(OR)_n$, new opportunities for changing the network are offered to the sol-gel chemists.

The authors are grateful to F. Taulelle and J. Maquet for NMR experiments, G. Chottard for Raman spectroscopy measurements, M. Lavergne and P. Beaunier for TEM micrographs.

References

- [1] C.J. Brinker and G.W. Scherer, *Sol-Gel Science* (Academic Press, New York, 1990).
- [2] J. Livage, M. Henry and C. Sanchez, *Prog. Solid State Chem.* 18 (1988) 259.
- [3] M. Henry, J.P. Jolivet and J. Livage, *Structure and Bonding* (Springer, Berlin, Heidelberg, 1991).
- [4] E. Matijevic, *Ann. Rev. Mater. Sci.* 15 (1985) 483.
- [5] H. Schmidt and B. Seiferling, *Mater. Res. Soc. Symp. Proc.* 73 (1986) 739.
- [6] H. Schmidt, *J. Non-Cryst. Solids* 73 (1985) 681.
- [7] C. Sanchez and M. In, *J. Non-Cryst. Solids* 147&148 (1992) 1.
- [8] E.H. Bunce, *J. Phys. Chem.* 18 (1914) 269.
- [9] W.C. Harris, J.W. Levin, *Advances in Raman Spectroscopy*, Vol. 1 (Heyden, London, 1972).
- [10] T.R. Griffiths and R.A. Anderson, *J. Chem. Soc., Faraday Trans. I* 80 (1984) 2361.
- [11] C.F. Baes and R.E. Mesmer, *The Hydrolysis of Cations* (Wiley Interscience, New York, 1976).
- [12] J. Mink and Y.A. Pentin, *J. Organomet. Chem.* 23 (1970) 293.
- [13] L.M. Epshtein, V.L. Foss, Y.T. Struchhov and L.A. Kazitsyna, *Zh. Strukt. Khim.* 8 (1967) 1027.
- [14] C. Sourisseau and B. Pasquier, *J. Organomet. Chem.* 39 (1972) 51.
- [15] R.P.J. Cooney and J.R. Hall, *Aust. J. Chem.* 25 (1972) 1159.
- [16] F.A. Johnson and W.D. Perry, *Organomet.* 8 (1989) 2646.
- [17] R.R. Miano and R.A. Plane, *Inorg. Chem.* 3 (1964) 987.
- [18] L.E. McCandlish and J.W. Macklin, *J. Organomet. Chem.* 99 (1975) 31.
- [19] J.A. Potenza, L. Zyontz and J. San Filippo Jr., *Acta Crystallogr.* B34 (1978) 2624.
- [20] M.M. Kreevoy, P.J. Steinwand and T.S. Straub, *J. Org. Chem.* 31 (1966) 4291.
- [21] J. March, *Advanced Organic Chemistry*, 3rd Ed. (Wiley Interscience, New York, 1985).
- [22] A.J. Bloodworth, *J. Organomet. Chem.* 23 (1970) 27.
- [23] B.E. Mann and B.F. Taylor, ¹³C NMR Data for Organometallic Compounds (Academic Press, London, 1981).
- [24] A.N. Nesmeyanov, V. Aleksanyan, L. Denisovich, Y. Nekrasov, E. Fedin, V. Khvostenko and I. Kritskaya, *J. Organomet. Chem.* 172 (1979) 133.
- [25] J.W. Macklin, *Spectrochim. Acta* 32A (1976) 1459.